Marine Environmental Research 188 (2023) 105997

Contents lists available at ScienceDirect

Marine Environmental Research

journal homepage: www.elsevier.com/locate/marenvrev

Spatial sedimentation and plant captured sediment within seagrass patches

Aina Barcelona [a,*], Jordi Colomer [a], Teresa Serra [a]

[a] Department of Physics, University of Girona, 17071, Girona, Spain

ARTICLE INFO

Keywords:
Seagrass
Sedimentation
Leaves capture
Suspension
Seagrass patch
Fragmentation

ABSTRACT

Habitat degradation in coastal ecosystems has resulted in the fragmentation of coastal aquatic vegetation and compromised their role in supplying essential ecological services such as trapping sediment or sequestering carbon. Fragmentation has changed seagrass architecture by decreasing the density of the canopy or engendering small patches of vegetated areas. This study aims to quantify the role different patch sizes of vegetation with different canopy densities have in the spatial distribution of sediment within a patch. To this aim, two canopy densities, four different patch lengths, and two wave frequencies were considered. The amounts of sediment deposited onto the bed, captured by plant leaves, remaining in suspension within the canopy, and remaining in suspension above the canopy were used to understand the impact hydrodynamics has on sediment distribution patterns within seagrass patches. In all the cases studied, patches reduced the suspended sediment concentrations, increased the capture of particles in the leaves, and increased the sedimentation rates to the bed. For the lowest wave frequency studied (0.5 Hz), the sediment deposited to the bottom was enhanced at canopy edges, resulting in spatial heterogeneous sedimentation patterns. Therefore, restoration and preservation of coastal aquatic vegetation landscapes can help face future climate change scenarios where an increase in sedimentation can help mitigate predicted sea level rise in coastal areas.

1. Introduction

The maritime coastal seascape has suffered from both short and long-term structural changes because of increased anthropogenic impacts, population growth in coastal areas, habitat degradation, and the increasing impact of climate change (Barsanti et al., 2007; Cacabelos et al., 2022; Leriche et al., 2006; Montefalcone et al., 2019; Valero et al., 2009; Van De Koppel, 2015). Coastal seagrass meadows have been losing coverage over time, resulting in an increasingly fragmented landscape configuration (Montefalcone et al., 2010; Barcelona et al., 2021b). Therefore, coastal seagrasses can form large continuous meadows or more heterogeneous structures with different sized patches of vegetated areas mixed with assorted unvegetated sand or rocky beds. When a continuous seagrass meadow loses some of its vegetated area, it transforms into patchier areas with unvegetated bare soil and exhibits increasing gaps within the vegetation itself. The ability of coastal canopies to deal with both natural and anthropogenic disturbances has become a challenge for coastal marine ecosystem management and conservation as coastal canopies display patchiness that can persist over extended time scales (Bell et al., 2001; Colomer and Serra, 2021; Montefalcone et al., 2010). Consequently, individual patches of vegetation are now a typical sight in seascapes (Barcelona et al., 2021a; Borfecchia et al., 2021; Hovel et al., 2021; Pastor et al., 2022). High meadow fragmentation levels result in low shoot density in the surrounding area near gaps (Barcelona et al., 2021b), indicating the degrading effect fragmentation has.

Continuous coastal canopies are known to supply numerous ecological services such as reducing storm surges and marine heat waves, preventing the erosion of coastal beds (Madsen et al., 2001; Verdura et al., 2021), promoting sediment accretion (Granata et al., 2001) and heterogeneous litter decomposition, impacting carbon sequestration rates (Ettinger et al., 2017), influencing estuarine geomorphology (Lera et al., 2019) as well as providing refuge and nursery grounds for the local biota (Bell et al., 2001). However, when coastal seagrasses are fragmented, their role in supplying ecological services has been reported to be increasingly compromised. The ensuing levels of deterioration depend on the degree of local patchiness and the abiotic impacts (Colomer et al., 2017). The rise in sea levels predicted by future climate change scenarios, coupled with the low input of sediments from rivers, are expected to drown deltas (Dunn et al., 2019). Restauration of aquatic vegetation landscapes is a sedimentation enhancing strategy that can be used to compensate rising sea levels (Cox. et al., 2022). More

* Corresponding author.
E-mail address: aina.barcelona@udg.edu (A. Barcelona).

https://doi.org/10.1016/j.marenvres.2023.105997
Received 15 February 2023; Received in revised form 11 April 2023; Accepted 13 April 2023
Available online 23 April 2023

rigid submerged structures like coral reefs are also known to enhance sediment accretion and offset the erosive effects of rising sea levels (Tuck et al., 2021). Therefore, to cope with future climate change scenarios, preserving aquatic vegetation among other coastal landscapes is of special relevance.

Within canopies habitat complexity generally increases not only from patch edges to patch interiors (Moore and Hovel, 2010), patch-to-patch interactions (Abadie et al., 2017; Cornacchia et al., 2019) and fragmented to full canopies (Colomer and Serra 2021), but also in sparse to dense vegetation (Barcelona et al., 2021a) and in the differing leaf configurations of submerged and emergent plants (Barcelona et al., 2021b; Colomer et al., 2017; Montefalcone et al., 2006). Coastal canopies provide high flow resistance, and flow and waves are diverted and intensified above and/or next to the canopy, thus increasing water velocity and turbulence along the boundaries of the patch (Chen et al., 2013; Sand-Jensen and Mebus, 1996; Sand-Jensen and Pedersen, 2008). The balance between flow inertia, canopy drag, and canopy patch dimension determines, for example, particle deposition, which is laterally uniform (Zong and Nepf, 2011) and decreases inside the canopy patch (Zhu et al., 2021), indicating that within a patch sedimentation increases.

Gacia and Duarte (2001) reported that *Posidonia oceanica* meadows significantly buffer sediment resuspension. For instance, within the patch, sediment resuspension is three-fold lower than an area of bare sand. In their study, Serra et al. (2020) observed that constant sedimentation rates were found across gaps (zones without vegetation) of different sizes within a *Posidonia oceanica* meadow. They also found that sedimentation rates in the gaps within the meadow were close to those inside the canopy. In salt marshes, patches of vegetation have been found to participate in the sequestration and longstanding accumulation of sediments before they are then transported to the ocean (Pinheiro et al., 2002). Deposition of particle fluxes in patches of the seagrass *Zostera noltii* have been found higher within the patch than on bare sediments, i.e., the greater the vegetation density is, the higher the deposition rates are (Ganthy et al., 2015). Likewise, dense *Zostera marina* patches promoted the accumulation of fine sediments and organic content, therefore producing muddification in the interior of the patch. van Katwijk (2010) found that dense vegetated patches presented homogeneous sedimentation distribution, whereas although sparse vegetated patches presented a heterogeneous distribution of sediment, there was a decrease in fine particles compared to coarse particles. However, turbidity currents travelling through dense vegetated patches presented heterogeneous distributions of sediment, with fine sediment particles accumulating in the interior of a patch and coarse particles in its exterior (Soler et al., 2021). Barcelona et al. (2021c) reported that seagrass meadows may also capture sediment on the blades and thus enhance particle sedimentation on the seabed. The number of particles trapped by the blades of seagrass plants, and subsequently deposited on the seabed, increased with canopy density which, in turn, reduced the concentration of sediments in suspension within the canopy, thus improving the water clarity within the canopy. The impact meadows have on particle deposition and resuspension depends on the degree of current and wave attenuation, indicating that patches of vegetation can reduce particle resuspension from the bottom seabed, and enhance particle deposition and carbon burial (Gacia and Duarte, 2001; Oreska et al., 2017; Paladini de Mendoza et al., 2018). Deforestation of mangrove forests has also been shown to reduce blue carbon sequestration, showing the role that large continuous vegetation landscapes can play in facing future climate change scenarios (Chatting et al., 2022).

Nevertheless, both small and sparse vegetated patch behaviour has been found to deviate from large, dense seagrass patches. Pastor et al. (2022) pointed out that once seagrass degradation reaches a tipping point, functionality is lost and patches transition to a bare soil steady state, thus compromising potential restoration. Furthermore, Sweatman et al. (2017) suggested that fragmented seagrass beds shift their nutrient loads, which subsequently impacts their ecosystem functions in many ways by, for instance, reducing the availability of suitable habitats for animals or altering the available resources. Seagrass habitat fragmentation has also been found to threaten carbon sequestration (Mazarrasa et al., 2018). Continuous meadows are expected to be more efficient sequestering carbon than fragmented meadows. Previous experiments on the hydrodynamics of vegetated patches under oscillatory flows demonstrate that a minimum patch size is required to reduce the flow velocity through the turbulent kinetic energy being produced by plant stems (Barcelona et al., 2021a). A patch that is too small is unable to reduce waves and presents scouring at the meadow's edges (Marin-Diaz et al., 2020). However, there is still a lack of knowledge concerning the capacity seagrass patches have to capture sediment from allochthon sources. Therefore, this current study attempts to acquire knowledge as to the effect patch length and canopy density can have on the capture of sediment from allochthon sources under different hydrodynamic conditions. The sediment captured by leaves, the sediment deposited at the bottom and the sediment remaining in suspension will be studied for small (five times the leaf length) to large (14 times the leaf length) vegetated patch lengths, for two canopy densities (dense and sparse) and two different wave frequencies. The study was performed in a laboratory flume under conditions mimicking real field scenarios.

2. Methodology

2.1. The flume

The study was carried out in a methacrylate laboratory flume 600 cm long, 50 cm wide and 60 cm deep (Fig. 1) with a mean water height of h = 30 cm. The flume was equipped with a vertical piston-type wavemaker at the entrance. The wavemaker was driven by a variable-speed motor at two frequencies (f = 0.5, and 1.12 Hz). To eliminate wave reflection, a plywood beach (slope = 1:2) covered with foam rubber was placed at the end of the flume (Barcelona et al., 2021a; Serra et al., 2018).

2.2. Patches of flexible vegetation

The vegetation model consisted of a series of flexible plants made from eight 0.075 mm-thick polyethylene canopy blades attached to PVC dowels that had been randomly inserted into a 250-cm long perforated

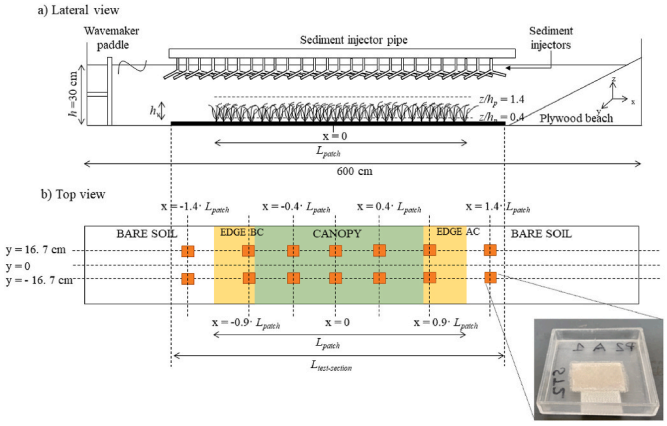

Fig. 1. Scheme of the experimental set-up a) Lateral view of the flume with the patch of flexible vegetation. The patch lengths ranged from L_{Patch} = 70–196 cm. b) Top view of the set-up. The region coloured in orange and green correspond to the patch. The green coloured area corresponds to the inner canopy region and the orange-coloured area corresponds to the edge region of the canopy. The Edge BC corresponds to the edge closest to the wavemaker and the Edge AC corresponds to the edge furthest from the wavemaker. Orange squares represent the sediment traps distributed along the flume bed.

baseboard (Pujol et al., 2013). PVC rigid dowels extended 1 cm above the bed (Zhang et al., 2018). The model plants were geometrically and dynamically close to *Posidonia oceanica* plants (Ghisalberti and Nepf, 2002). Leaf length, h_p, was 14 cm, and the effective height when the leaves were bent by the waves was $h_v = 8.4$ cm for $f = 1.12$ Hz and $h_v = 10.5$ cm for $f = 0.5$ Hz (Barcelona et al., 2021a). The vegetation density of patches was quantified using the solid plant fraction (*SPF*) defined as:

$$SPF\ (\%) = 100n\pi\left(\frac{d}{2}\right)^2 \quad (1)$$

where n is the number of shoots per unit area and d is the stem diameter (1 cm). Three SPFs were used (0%, 3.5% and 10%), which corresponded to vegetation densities of n = 0, 446 and 1273 stems·m^{-2}, according to the range of canopy densities (78–1000 stems·m^{-2}) found in coastal areas (Bacci et al., 2017; Boström et al., 2014; Colomer et al., 2017; Gera et al., 2013). *SPF* = 0% corresponded to the non-vegetated set-up. For each *SPF*, four patch sizes, L_{patch}, ranging from 70 to 196 cm in length were considered. A total of 18 experiments were performed for the different *SPFs*, L_{patch} and f (Table 1).

2.3. Sediment injection

The sediment used in the experiments was a synthetic dust powder (ISO 12103–1. A4 Coarse, Powder Technology Inc. Burnsville) with a median of 41.7 μm (Fig. 2) and a density of 2650 kg m^{-3}. The mean settling velocity for these sediment particles ($w_{settling} = 1.57 \times 10^{-3}$ m s^{-1}) was estimated by the Francalaci et al. (2021) formula assuming that sediment particles were nearly spherical (i.e., with a Corey shape factor equal to 1). Since the suspended sediment concentration in all the experiments was below 17.46 g L^{-1}, the sediment concentration was not expected to have any effect on the settling velocity (Colomer et al., 1998). The volumetric concentrations of suspended sediment (in μL·L^{-1}) were analysed using a LISST-100X (Laser In-Situ Scattering and Transmissometry, Sequoia Scientific, Inc, Bellevue, WA) particle size analyser. The LISST-100X consists of a laser beam and an array of detector rings of progressive diameters which allow the light received at the scattering angles of the beam to be analysed. The device measures particle volume concentrations for 32 size classes (logarithmically distributed in the size range of 2.5–500.0 μm), using the procedure based on the diffraction theory of light. This instrument has been widely used for organic (Serra et al., 2001) and inorganic particles (Ros et., 2014; Serra et al., 2002). The particle size distribution of the sediment used was bimodal, with fine particles being 2.5–6.0 μm in diameter, i.e., corresponding to strongly cohesive clay and very fine silts, and coarse particles were 6.0–122.0 μm in diameter, i.e., corresponding to weakly cohesive fine to coarse silts and small sand particles (Fig. 2). In this case, $d_{50} = 41.7$ μm, is of the order of the grain size of river plumes in coastal areas (40–65 μm, Pitarch et al., 2019). Pitarch et al. (2019) found that the largest non-cohesive particles settled at the mouth of the river and the finest sediment fractions were transported offshore.

The wavemaker was switched on and left to run for 15 min to allow

Table 1
Summary of the experimental conditions considered: each experimental run number (with the seagrass flexible vegetation as *SFV*), wave frequency (f, in Hz), solid plant fraction (*SPF*, in %), canopy density (n, in shoots m^{-2}), length of the vegetated patch (L_{patch}, in times the leaf length h_p), U_w (in cm s^{-1}) at $z/h_v = 0.4$ and the ratio between the orbital excursion length (A_w), and plant-to-plant distance (S).

Run	f (Hz)	*SPF* (%)	N (stems·m^{-2})	L_{patch}/h_p	U_w at $z/hv=0.4$ (cm s^{-1})	Aw/S
SFV 1	0.5	0	0		8.95	
SFV 2		3.5	446	0.36	9.40	0.63
SFV 3				0.64	9.37	0.63
SFV 4				0.86	8.93	0.60
SFV 5				1.00	9.22	0.62
SFV 6		10	1273	0.36	9.42	1.07
SFV 7				0.64	9.16	1.04
SFV 8				0.86	9.26	1.04
SFV 9				1.00	9.07	1.03
SFV 10	1.12	0	0		8.21	
SFV 11		3.5	446	0.36	8.33	0.25
SFV 12				0.64	7.99	0.24
SFV 13				0.86	8.02	0.24
SFV 14				1.00	8.01	0.24
SFV 15		10	1273	0.36	8.29	0.42
SFV 16				0.64	7.88	0.40
SFV 17				0.86	7.80	0.40
SFV 18				1.00	7.70	0.39

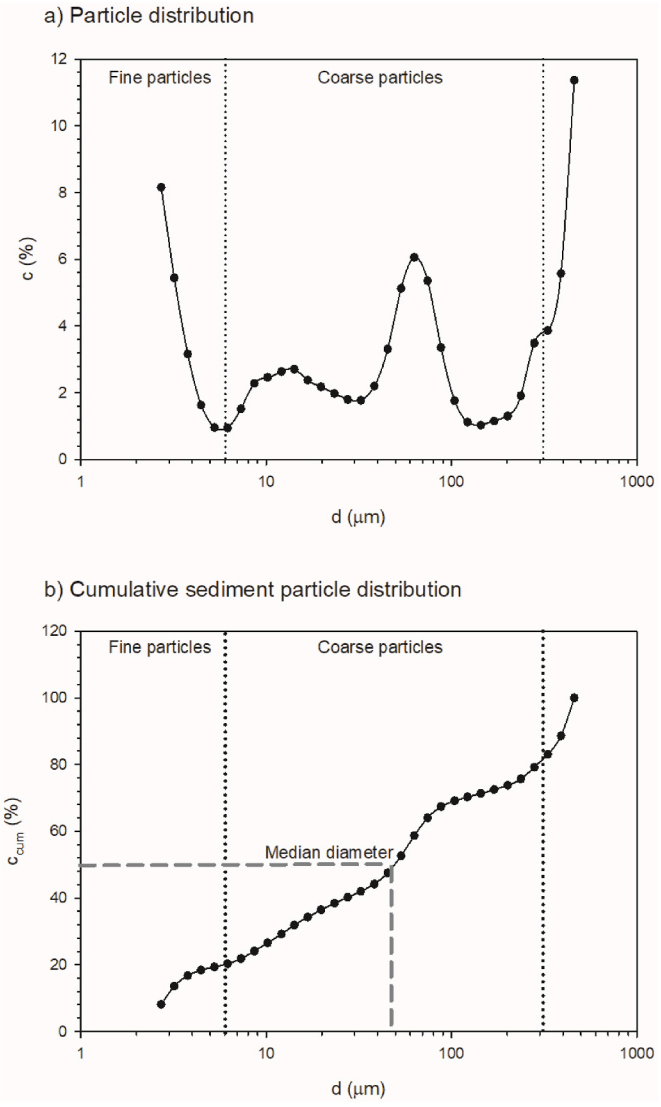

Fig. 2. a) Volumetric sediment particle size distribution (c, in %). b) Cumulative sediment particle size distribution (c_{cum}, in %). Dashed lines show the median diameter (i.e., the diameter where 50% of the cumulative distribution holds, $d_{50} = 41.7$ μm). In both figures, two different particle sizes are shown: fine particles below 6 μm, and coarse particles between 6 μm and 122 μm.

the system to reach equilibrium before sediment injection. The particle-laden flow used in the injection was prepared using an initial volume (2L) of sediment suspension (with a concentration of 80 g L^{-1}) and introduced into one end of the sediment-injector pipe. The injector pipe was situated at y = 0 cm along the axis of the flume (Fig. 1) While introducing the sediment into the pipe, the injectors faced upwards to avoid any uncontrolled spillage. Once the pipe had been filled with the sediment suspension, it was then closed and turned down so that injectors face downwards, protruding 5 cm below the water surface and therefore remaining at the very top of the water column and above the vegetated patch.

The sediment injector pipe consisted of a large 2.5 m-long pipe, with 42 sediment injectors evenly distributed 7 cm apart from each other. The Y-shape design of the sediment injectors was 26 cm long and each arm pipe was 22.5 cm long (see Fig. 1a). Each arm of the pipe had 12 holes, from where the sediment injected was released into the flume, thus resulting in a homogeneous injection along both the x-axis and the y-axis.

2.4. Sediment measurements

To obtain the sediment particle distribution along the canopy, three different types of sediment measurements were collected: sediment settled on the bed, suspended sediment, and sediment attached to plant leaves. To obtain the amount of sediment settled on the bed, fourteen sediment traps were distributed in two rows along the main axis of the flume and situated at y = ±16.7 cm (Fig. 1b). The traps' positions along the x-axis of the flume for each run were related to the patch length, x = ± 0, 0.4, 0.9 and 1.4·L_{patch} (Fig. 1b). Sediment traps were distributed into three subgroups: canopy, corresponding to the traps at x = ± 0 and 0.4·L_{patch}; edge, corresponding to the traps at x = ± 0.9·L_{patch}; and bare soil, corresponding to the traps outside the vegetated patch at x = ± 1.4·L_{patch}. The sediment samples from the sediment traps were collected at t = 60 min from the injection time. In order to obtain information on the suspended sediment, 80 mL of suspended sediment samples were pipetted at the same x position where the sediment traps were positioned for each run, at y = 0 cm, and at two water depths (at $z/h_v = 0.4$ and at $z/h_v = 1.4$). These samples were chosen as representative samples for within and above the canopy, respectively. In this case, samples were collected at different times (t = 2, 30 and 60 min) from the injection time, and analysed for suspended sediment concentration. To obtain information about the amount of sediment deposited on the plant leaves, at the end of each experiment (t = 60 min) five plants were gently removed at the same x positions within the vegetated patch as the sediment traps had been placed. They were then introduced into a beaker with 80 ml of water and the plants were stirred in the fluid to remove the sediment trapped by the surface of the leaves, after which particle concentration was analysed with the particle analyser LISST-100X.

2.5. Sediment capture distribution analysis

To calculate the amount of sediment collected in the different compartments of the system, a test section of 14h_p was considered. In other words, it coincided with the longest patch studied (see Fig. 1). The test section had different configurations depending on the presence or absence of vegetation. In the cases with vegetation, patch length and canopy density determined the amount of vegetation in the system. The test section had a vegetated vertical region within the canopy and an unvegetated vertical region above the canopy. In the non-vegetated experiments, the same two vertical layers were considered for the purpose of comparison.

The sediment trapped by the leaves, V_P (Fig. 3), corresponded to the sediment attached to the surface of the plant leaves. The concentration of sediment measured with the LISST -100x was divided by the number of plants collected for sampling and the volumetric concentration of sediment collected per plant was obtained. The concentration obtained was afterwards multiplied by the volume of the water used to rinse the plants (80 mL) and the total volume of sediment deposited was obtained (V_P, in μL).

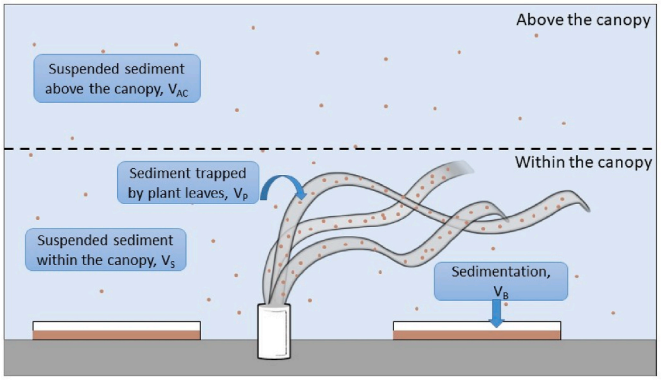

Fig. 3. Distribution of sediment in the four different compartments: on the plants (V_P), on the bed (V_B), in suspension within the canopy (V_S) and in suspension above the canopy (V_{AC}).

The amount of sediment in suspension within the canopy (V_S, Fig. 3) was calculated from the samples collected in suspension at a 5 cm depth above the bottom of the flume. The same depth was considered for the non-vegetated cases. For experiments carried out with vegetation, the test section had a vegetated part and a bare soil part. The volume of particles in suspension (V_S, in μL) was calculated by multiplying the concentration within the canopy by the volume of the patch ($L_p \times h_v \times$ W, where W is the width of the flume) plus the concentration in suspension in the bare soil multiplied by the volume of sediment collected in the bare soil (($L_{test\text{-}section}$-L_p) × h_v × W). In the case without vegetation, the volume of sediment in suspension was calculated by multiplying the concentration of sediment in suspension by the volume of the test section ($L_{test\text{-}section} \times h_v \times W$). The same calculation was carried out for the suspended sediment concentration above the canopy (at 20 cm above the bottom, V_{AC}, in μL). However, the vertical extension in this case was (h-h_v) instead of h_v used for the within canopy section.

The amount of sediment deposited at the bottom of the flume (V_B, in μL, Fig. 3) was calculated from the samples collected with the sediment traps. The concentration of sediment collected by the sediment traps was measured by the LISST-100X. The volume of sediment was obtained by multiplying the concentration obtained by the volume of the sample. Since the volume of sediment obtained corresponded to the area of the sediment trap (5 cm × 5 cm), the total volume of sediment deposited in the region where the trap was positioned was obtained by multiplying by the ratio of the total area of the region where the trap was situated (edge, bare soil, or vegetation) divided by the area of the test section. The total volume of sediment (V_B) at the bottom of the test section was calculated as the sum of the volume of sediment collected at the bottom of the bare soil plus the sediment collected at the edge and the sediment collected at the canopy regions.

The total volume of sediment was obtained by adding the volume of particles for each compartment in the test section (V_{TOTAL}=V_P + V_{AC} + V_S + V_B). From the total volume, the percentage of sediment particles in each compartment was calculated.

2.6. Measuring velocities

The Eulerian velocity field was defined as (u, v, w) in the (x, y, z) directions of the flume, respectively. The three components of velocity were recorded with a downwards looking Acoustic Doppler Velocimeter (16-MHz MicroADV, Sontek) at a frequency of 50 Hz over 10 min (obtaining a set of 30,000 data for each sampling point). Flow velocity profiles were measured at the centre of the patch and at z = 17 cm, 16

cm, 12 cm, 8 cm, 6 cm, 5 cm, 4 cm, 3 cm, and 2 cm from the bed of the flume. The ADV measures 5 cm from the probe tip with a sampling volume of 0.09 cm^3. Beam correlations less than 80% were discarded and spikes were removed (Goring and Nikora 2002; Pujol et al., 2013). For oscillatory flows, the instantaneous velocity, $U_i(t)$, can be decomposed as:

$$U_i(t) = U_c + U_w + u' \quad (2)$$

where U_c is the steady velocity associated with the current, U_w is the unsteady wave motion which represents spatial variations in the phase-averaged velocity field, and u' is the turbulent velocity, that is, the instantaneous velocity fluctuation in the x-direction. U_c is the phase-averaged velocity:

$$U_c = \frac{1}{2\pi}\int_0^{2\pi} U_i(\varphi)\partial\varphi \quad (3)$$

where $U_i(\varphi)$ is the instantaneous velocity according to the phase (Lowe et al., 2005b; Luhar et al., 2010). In the current study U_c at $z/h_v = 0.4$ above the bed (i.e. within the canopy layer) was always smaller than U_w, with mean values of 0.44 cm s^{-1} and -0.05 cm s^{-1} for the wave frequencies of 1.12 Hz and 0.5 Hz, respectively.

Wave velocity, U_w, was obtained by using a phase averaging technique. The Hilbert transform was used to average oscillatory flow velocities with a common phase (Pujol et al., 2013b; Ros et al., 2014). The root mean square (rms) of $U_i(\varphi)$ was considered as the characteristic

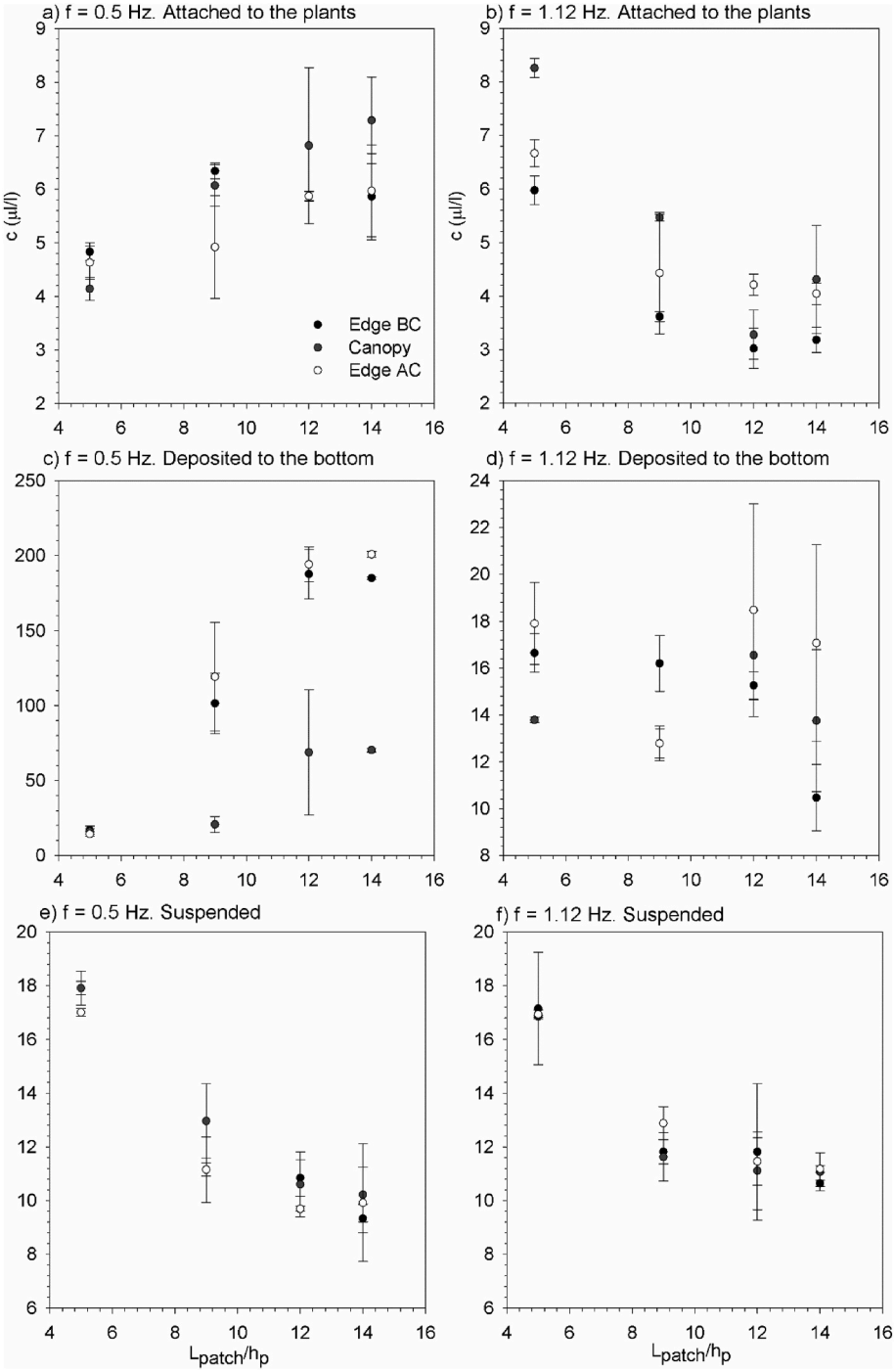

Fig. 4. Sediment concentration, c, trapped by the plant leaves vs. the ratio between patch length and plant height, L_{patch}/h_p for experiments carried out at SPF = 3.5%. Blue circles correspond to measurements taken at the edge BC (Fig. 1); red circles to the measurements taken in the inner canopy area; and unfilled circles to the measurements taken at the edge AC (Fig. 1). For a) f = 0.5 Hz and for d) f = 1.12 Hz. Sediment concentration, c, deposited at the bottom of the flume vs. L_{patch}/h_p, for b) f = 0.5 Hz and for e) f = 1.12 Hz. Suspended sediment concentration, c, remained in suspension within the canopy at z/h_p = 0.4, for c) f = 0.5 Hz and for f) f = 1.12 Hz.

value of the orbital velocity U_w^{rms} (U_w hereafter) at each depth, and was calculated according to:

$$U_w^{rms} = \sqrt{\frac{1}{2\pi}\int_0^{2\pi} (U_i(\varphi) - U_c)^2 \partial\varphi} \quad (4)$$

2.7. Theory

A non-dimensional model was constructed based on the Pi-Buckingham theorem. Four main variables and two dimensions were considered in this current study. The variables are the wave excursion length ($A_w = U_w/(2\pi f)$), the plant-to-plant distance ($S = n^{-1/2}$), the patch length (L_p) and the effective vegetation height (h_v). The effective vegetation height is the height of bent plants when they swing with the flow and will depend on the wave frequency (Barcelona et al., 2021c, 2023). The two dimensions are metres and seconds. Therefore, two governing non-dimensional parameters can be constructed to describe the results. First, A_w/S, i.e., the ratio between the wave excursion length and the plant-to-plant distance, accounts for the penetration of the wave within the vegetated patch. And second, L_p/h_v, which is the ratio between the length of the patch, L_p and the effective vegetation height h_v. Based on the above governing parameters, it is possible to expect that the percentage of sediment trapped by the leaves, the sediment in suspension and the sediment settled at the bottom of the tank, is a function of the dimensionless parameters, A_w/S and L_p/h_v (Zong and Nepf, 2011).

3. Results

After 60 min (from injection) had lapsed, the concentration levels of the sediment in suspension reached a steady state. In this steady state, the injected sediment was distributed into the four regions considered (Fig. 3): attached to the plant leaves, deposited at the bottom of the flume, or in suspension either above or within the canopy.

For each wave frequency considered, the concentration of particles trapped by individual plant leaves did not differ between the different regions (canopy and edges) (Fig. 4a and b). However, the behaviour of the sediment concentration with L_p/h_v was different depending on wave frequency. For the lower frequency (f = 0.5 Hz), the longer the patch length, the greater the amount of sediment trapped on the leaves (Fig. 4a). In contrast, for the highest frequency (f = 1.12 Hz), the longer the patch length, the lower the amount of sediment trapped by plant leaves (Fig. 4b).

The sediment concentration deposited at the bottom behaved differently depending on wave frequency. For the lowest wave frequency (f = 0.5 Hz), an increase in the patch length resulted in an increase in the sediment deposited at the bottom. Likewise, lower sediment concentrations were found within the canopy instead of at the edges (Fig. 4c). Meanwhile, for the highest frequency (f = 1.12 Hz), the sediment deposited at the bottom remained constant for all the patch lengths studied (Fig. 4d). In addition, for this wave frequency, there were no differences in sediment concentration levels between the edges and the canopy (Fig. 4d).

The suspended sediment concentration levels presented the same behaviour for the two wave frequencies studied: f = 0.5 and 1.12 Hz. The greater the patch length, the lower the sediment concentration that remained in suspension. In this case, there were no differences in suspended sediment concentration levels between the edge and the canopy (Fig. 4e and f).

Furthermore, it must be noted that, although both the sediment deposited on the leaves and the sediment remaining in suspension had the same range for the two wave frequencies studied (Fig. 4a, b, e and f), the range of the amount of sediment deposited at the bottom for f = 0.5 Hz was ten times that for f = 1.12 Hz (Fig. 4c and d).

The dependence of the percentage of the volume of sediment particles trapped by the leaves, V_P, with the non-dimensional parameter (A_w/S)/(L_p/h_v) presented two regimes (Fig. 5). For (A_w/S)/(L_p/h_v) < 8, a first regime where V_P remained constant with (A_w/S)/(L_p/h_v) with V_P = 4.7%. However, for (A_w/S)/(L_p/h_v) > 8, V_P increased linearly with (A_w/S)/(L_p/h_v) (Fig. 5). The first regime (left part of Fig. 5) mainly corresponded to cases with the highest frequency (f = 1.12 Hz). In contrast, the second regime (right part of Fig. 5) corresponded mainly to the experiments carried out with the lowest frequency (f = 0.5 Hz), independent of the canopy density.

The volume of particles remaining in suspension (in %) within the canopy was found to decrease linearly with (A_w/S)/(L_p/h_v) (Fig. 6).

The volume of the sediment deposited at the bottom (V_B, in %) versus (A_w/S)/(L_p/h_v) presented two regimes (Fig. 7). A first regime for (A_w/S)/(L_p/h_v) < 8, where V_B remained constant with (A_w/S)/(L_p/h_v) with V_p = 22.6%. A second regime for (A_w/S)/(L_p/h_v) > 8, where V_P increased linearly with (A_w/S)/(L_p/h_v) (Fig. 7). As with V_P, the first regime (left part of Fig. 7) mainly corresponded to the cases carried out with the highest frequency (f = 1.12 Hz) and the second regime (right part of Fig. 7) to the experiments carried out with the lowest frequency (f = 0.5 Hz).

4. Discussion

The current study demonstrates that both the architectural structure of a seagrass patch and the hydrodynamics impact sediment distribution. That is, the amount of sediment deposited on the bed and plant leaves, and the suspended sediment presents different percentages depending on the structural characteristics: patch length and plant density, and on the hydrodynamics, here the through-the-wave frequency.

Plant leaves captured sediment with a concentration that did not differ between whether the plants were situated within the canopy or at the edges of the canopy. However, it is interesting to notice that the sediment concentration captured by plant leaves increased with the

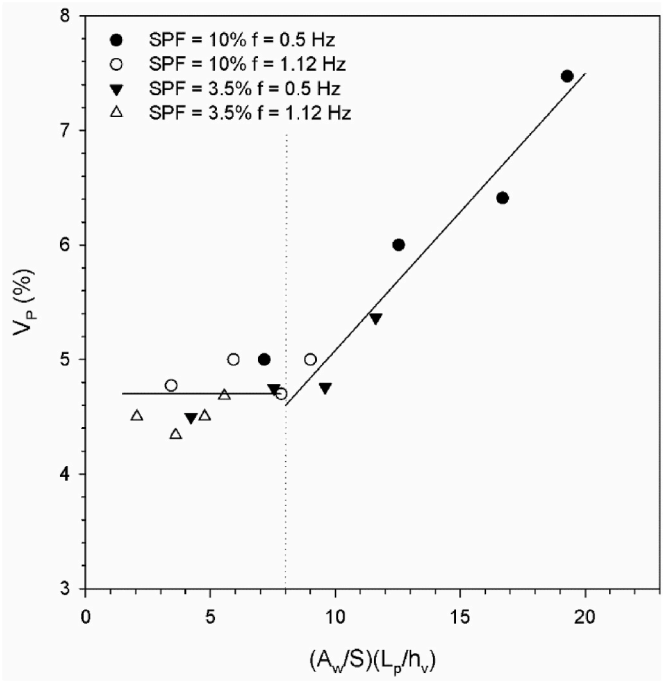

Fig. 5. Relationship between the volume of sediment trapped by the leaves, V_P, and (A_w/S)/(L_p/h_v) for all the experiments carried out. The vertical dashed line represents the minimum value of (A_w/S)/(L_p/h_v) that separated the different behaviours observed. The horizontal solid line at V_P = 4.7% represents the mean value of V_P for (A_w/S)/(L_p/h_v) < 8, where the V_P remained constant. For (A_w/S)/(L_p/h_v) > 8 a linear tendency was found with $V_P = 0.17 * (A_w/S)/(L_p/h_v) + 3.31$, with $R^2 = 0.80$ and 95% of confidence.

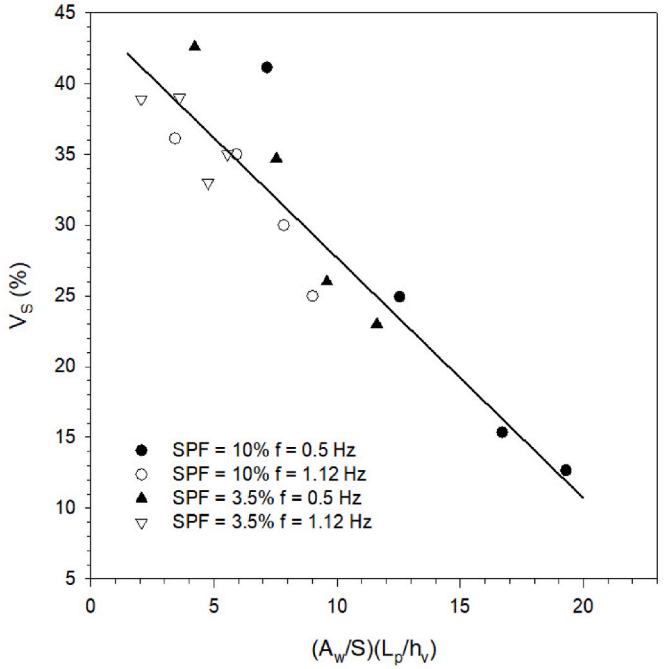

Fig. 6. Relationship between the sediment that remained in suspension, Vs, for all the experiments carried out. The solid line represents the linear tendency that was found Vs = −1.76 * $(A_w/S)/(L_p/h_v)$ + 44.60, with R^2 = 0.88 and 99% of confidence.

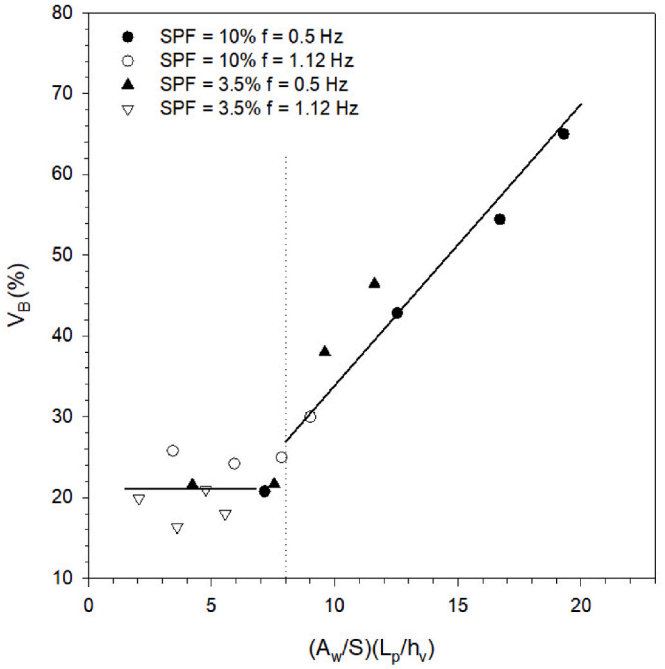

Fig. 7. Relationship between the volume of sediment deposited at the bottom, V_B, for all the experiments carried out. The vertical dashed line represents the minimum value of $(A_w/S)/(L_p/h_v)$ that separated the different trends observed for the V_B. The horizontal solid line at V_B = 22.58% represents that for $(A_w/S)/(L_p/h_v) < 8$, where the V_B remained constant. For $(A_w/S)/(L_p/h_v) > 8$, a linear tendency was found $V_B = 3.15^*$ $(A_w/S)/(L_p/h_v)$+ 3.92, with R^2 = 0.95 and 99% of confidence.

patch size for the wave frequency of 0.5 Hz and decreased with the patch size for 1.12 Hz. This difference might be because plants in large seagrass patches and low frequency wave environments have a large swing movement with a greater stroke, which would increase the chance of sediment particles being captured by single plants. On the other hand, the fast movement of the plant leaves in large seagrass patches and under a wave frequency of 1.12 Hz may increase the friction between leaves and cause the ejection of particles, thus reducing the chance of particles being potentially captured by plant leaves (Barcelona et al., 2021c).

Sediment particles deposited on the bottom also presented different behaviours depending on the wave frequency. In wave frequency environments of 0.5 Hz, plants in large seagrass patches played a synergistic role, consequently increasing by nearly ten times, the amount of sediment deposited onto the bottom from the smaller patch of $5h_p$ up to the largest patch of $14h_p$. In this case, sedimentation was maximized at the edges of large patches. This result agrees with those of Navarrete-Fernández et al. (2022) who found that microparticles presented the maximum sedimentation rates at the edges of the canopy, while decreasing towards the inner canopy. Zong and Nepf (2011) also found a heterogeneous distribution of sediment deposition in a patch of vegetation in a unidirectional flow. In their case, high deposition rates were observed at the edge of dense patches of vegetation, while also decreasing towards the patch interior. The sedimentation within the vegetation obtained for the case of wave frequencies of 1.12 Hz, was also lower than that for wave frequencies of 0.5 Hz. This can be attributed to the different movements of waves of different frequencies. In the case of 0.5 Hz, plants moved back and forth. In contrast, in the case of 1.12 Hz, plants were bent and oscillated asymmetrically to one side (see videos in the Supplementary Material). The different movements could cause different boundary layers for the different wave frequencies. Measurements of the suspended particle concentration levels above the canopy reveal that for the frequency of 0.5 Hz the suspended concentration levels was 25% lower than for 1.12 Hz. Therefore, the low sedimentation associated to 1.12 Hz could be because more particles accumulate above the canopy than in the case of 0.5 Hz. The different behaviour of the vegetation under different wave frequencies results in different boundary conditions being produced by the plants which can also explain why 0.5 Hz presents heterogeneous horizontal patterns compared 1.12 Hz, where a horizontal homogeneous sedimentation pattern holds. Likewise, note that the sediment concentration obtained in the non-vegetated experiment was 15.0 μL L^{-1}, i.e., close to that obtained for the small patch of $5h_p$. This indicates that the effect of the small patch of $5h_p$ on sedimentation does not deviate much from the non-vegetated case. This result is in accordance with the findings by Colomer et al. (2017), who found that $6.6h_p$ patches of *Posidonia Oceanica* produce low sheltering of the bed, i.e., close to bare soil conditions.

Under a wave frequency of 1.12 Hz, the concentration of sediment deposited onto the bottom for all the patches studied was close to that obtained for the smallest patch with the lower wave frequency, and to the sedimentation for the non-vegetated case for that same wave frequency (11.0 μL L^{-1}). Contrary to the wave frequency of 0.5 Hz, under the wave frequency of 1.12 Hz, the concentration of sediment deposited at the bottom of the patch did not depend on patch length. In this case, the sediment concentration was distributed homogeneously throughout the patch without any differences between canopy edges and the inner region. Therefore, the impact of a seagrass patch on the sedimentation rates also depends on the hydrodynamics of the flow, with heterogeneous distribution in wave frequencies of 0.5 Hz, and homogeneous distribution in wave frequencies of 1.12 Hz.

Contrary to what has been observed for the flux of sediment to the bottom and the capture of sediment by plant leaves, suspended sediment presents the same behaviour under both wave frequencies, 0.5 Hz and 1.12 Hz. In both cases, an increase in the patch length caused a decrease in the concentration levels of suspended sediment within the canopy. In addition, the suspended sediment concentration levels for the 1.12 Hz wave frequency was close to that obtained for 0.5 Hz. Therefore, the water quality within the patch, through a reduction in particle concentration, improves as the length of the patch increases. It must also be

noted that under both frequencies no differences in suspended sediment concentration levels were observed between canopy edges and patch interiors. The suspended sediment concentration ranged between 10 μL L^{-1} to 18 μL L^{-1}. The density of the sediment used in the current study was 2650 kg m^{-3}, which resulted in a suspended sediment concentration of 45 mg L^{-1}. This concentration is within the concentration range of river sediment plumes in natural environments (Tassan, 1997; Warrick et al., 2004; Liu et al., 2022).

The percentage of particles captured by plant leaves was nearly constant 4.7% versus the non-dimensional parameter (A_w/S) (L_p/h_v) up to a threshold of (A_w/S) $(L_p/h_v) = 8$. For (A_w/S) $(L_p/h_v) > 8$, the percentage of particles captured by plant leaves increased linearly with (A_w/S) (L_p/h_v). This second region indicates that more sediment particles are captured by plant leaves when A_w/S or L_p/h_v increase. The volume of sediment deposited on the bed presents the same threshold at (A_w/S) $(L_p/h_v) = 8$, from where the percentage of sedimentation increases with (A_w/S) (L_p/h_v) for (A_w/S) $(L_p/h_v) > 8$. In contrast, for (A_w/S) $(L_p/h_v) < 8$ the percentage of deposited particles on the bed remains constant at its lowest value of 22.6%, indicating that the vegetated patch does not produce any effect on the sedimentation.

For $A_w/S > 0.35$, seagrass patches dissipate wave velocity by generating turbulent kinetic energy (Barcelona et al., 2023). In this regime seagrass patches behave like canopies, in contrast, for $A_w/S < 0.35$ seagrass patches present a single stem-like behaviour and do not generate turbulent kinetic energy. In the current study, all cases with $A_w/S > 0.35$ correspond to (A_w/S) $(L_p/h_v) > 8$, where the seagrass patch has the role of both increasing sediment capture by plant leaves and sedimentation at the bottom. Therefore, from the results of the current study, seagrass patches behave as canopies when (A_w/S) $(L_p/h_v) > 8$. This case is expected to hold for both high A_w/S or L_p/h_v. High values of A_w/S indicate that waves interact with the canopy dissipating the mean energy of the flow, and it also means that the orbital excursion length of the wave is greater than the plant to plant distance. Therefore, the canopy protects the bed from the oscillatory flow. L_p/h_v represents the longitudinal extension of the vegetated patch. The larger the patch, the greater its effect on the bed will be. This result agrees with Zhu et al. (2021) who observed that seagrass meadows trapped sediment due to the reduction of the mean energy of the flow (waves and currents). They observed this result when seagrass meadow density was high. *Posidonia oceanica* seagrasses have been found to increase the deposition of sediment particles compared to bare soil (Gacia and Duarte, 2001). In their work, waves of frequencies between 0.33 s^{-1} and 0.07 s^{-1} lead to bed orbital velocities of 2–10 cm s^{-1}, and mean shoot densities of 200 shoots m^{-2}, resulting in $A_w/S = 0.672 > 0.35$. Therefore, this case corresponds to the case of a canopy that reduces the mean energy of the flow through the production of turbulent kinetic energy and, in turn, enhances the deposition of sediment to the bed.

Therefore, the current study demonstrates that the threshold for when a seagrass patch of length L_p preserves canopy characteristics depends on the hydrodynamics (through A_w), the seagrass density (through S) and the effective plant height h_v, which, in turn, depends on the hydrodynamics and the plant flexibility. From the current study, small patches of vegetation produce a low deposition of sediment on the bottom and on their leaves, thus presenting a high suspended sediment concentration. These patches of vegetation are expected to be more vulnerable under adverse conditions. These results might also explain how an increase in patchiness leads to small fragmented *Zostera marina* seagrass patches of 5.6–10 m long disappearing due to anthropogenic pressures (García-Redondo et al., 2019). Olesen and Sand-Jensen (1994) observed high rates of *Zostera marina* mortality for small and sparse seagrass patches. Moreover, López-y-Royo et al. (2011) used ecological indicators to categorize the water quality in the evolution of *Posidonia oceanica*. In their study, low water quality was associated with *Posidonia oceanica* densities below 200 shoots m^{-2}. The current study demonstrates that for a sparse canopy to provide the required ecological services compared to a dense canopy, it must have a large patch. Therefore, the current study highlights the fact that canopy density is not the only crucial parameter indicating meadow quality, as so too does the length of the seagrass patch. Long and continuous seagrass meadows are expected to provide seabed sediment stabilization and boost sediment trapping, thus providing a sediment enhancing strategy to cope with future sea level rises or improve carbon sequestration levels.

5. Conclusions

The current study demonstrates the role seagrass patch length plays in distributing sediment within the patch itself. Patches of vegetation decreased the amount of suspended sediment concentration, compared with continuous vegetation landscapes. The larger and denser the patch is, the lower the concentration levels of suspended sediment are. This reduction in the suspended sediment concentration is caused by two mechanisms: the trapping of sediment particles by plant leaves and the enhancement of sedimentation by the presence of vegetation. From the current study, a seagrass patch is able to increase the settling of particles to the bottom and also to capture particles on their leaves provided (A_w/S) $(L_p/h_v) > 8$. This condition holds for both large or dense seagrass patches and provides the limit for when seagrass patches become vulnerable to external pressures. From the results presented here, information can be obtained concerning the minimum length and density a vegetated patch under certain hydrodynamics has to have to maintain the functionality of its canopy and thus be less vulnerable.

The current study demonstrates that seagrass patches in wave frequencies of 0.5 Hz present greater sediment deposition at the edges compared to the inner canopy region, resulting in spatial heterogeneous sediment deposition patterns. In contrast, sediment deposition rates in seagrass patches in wave frequency environments of 1.2 Hz present a spatial homogeneous distribution.

This study presents the behaviour of a seagrass patch from the perspective of the sediment distribution patterns in the vegetated patch. The results indicate when a seagrass patch is no longer able to modify sediment distribution patterns or ensure the stabilization of the bed, thus losing part of its functionality. It also demonstrates the vulnerability of small and sparse seagrass patches under external pressures. This study provides information on the vital role aquatic vegetation plays in enhancing sedimentation within the canopy. Preserving the vegetation in these seascapes can help mitigate the future climate change scenarios that predict a decrease in the retention of sediments in coastal areas and the erosion and shrinking of deltas. Likewise, continuous seagrass landscapes fragmentation also predicts a reduction in the sedimentation and, therefore, a reduction in the carbon burial.

CRediT authorship contribution statement

Aina Barcelona: Conceptualization, Data curation, Formal analysis, Methodology, Writing-original draft, Writing-review & editing. Jordi Colomer: Conceptualization, Data curation, Writing-review & editing. Teresa Serra: Conceptualization, Writing-review & editing, Funding acquisition, Supervision.

Declaration of competing interest

The authors declare that they have no known competing financial interests or personal relationships that could have appeared to influence the work reported in this paper.

Data availability

Data will be made available on request.

Acknowledgments

This project has been funded by the Ministerio de Ciencia e

Innovación of the Spanish Government through the grant PID 2021-123860O3-100. Aina Barcelona was founded by the pre-doctoral grant 2020 FI SDUR 00043 by the "Generalitat de Catalunya".

Appendix A. Supplementary data

Supplementary data to this article can be found online at https://doi.org/10.1016/j.marenvres.2023.105997.

References

Abadie, A., Borges, A.V., Champenois, W., Gobert, S., 2017. Natural patches in *Posidonia oceanica* meadows: the seasonal biogeochemical pore water characteristics of two edge types. Mar. Biol. 164, 166. https://doi.org/10.1007/s00227-017-3199-5.

Bacci, T., Rende, F.S., Scardi, M., 2017. Shoot micro distribution patterns in the Mediterranean seagrass *Posidonia oceanica*. Mar. Biol. 164, 85. https://doi.org/10.1007/s00227-017-3121-1.

Barcelona, A., Oldham, C., Colomer, J., Serra, T., 2021a. Functional dynamics of vegetated model patches: the minimum patch size effect for canopy restoration. Sci. Total Environ., 148854 https://doi.org/10.1016/j.scitotenv.2021.148854.

Barcelona, A., Colomer, J., Soler, M., Gracias, N., Serra, T., 2021b. Meadow fragmentation influences *Posidonia oceanica* density at the edge of nearby gaps. Estuar. Coast Shelf Sci. 249, 107106 https://doi.org/10.1016/j.ecss.2020.107106.

Barcelona, A., Oldham, C., Colomer, J., Garcia-Orellana, J., Serra, T., 2021c. Particle capture by seagrass canopies under an oscillatory flow. Coast. Eng. 169, 103972 https://doi.org/10.1016/j.coastaleng.2021.103972.

Barcelona, A., Colomer, J., Serra, T., 2023. Stem stiffness functionality in a submerged canopy patch under oscillatory flow. Sci. Rep. (in press).

Barsanti, M., Delbono, I., Ferretti, O., Peirano, A., Bianchi, C.N., Morri, C., 2007. Measuring change of coastal biodiversity: diachronic mapping of the meadow of the seagrass *Cymodocea nodosa (ucria) ascherson* in the gulf of tigullio (ligurian sea, NW mediterranean). Hydrobiologia 580, 35–41. https://doi.org/10.1007/s10750-006-0467-7.

Bell, S.S., Brooks, R.A., Robbins, B.D., Fonseca, M.S., Hall, M.O., 2001. Faunal response to fragmentation in seagrass habitats: implications for seagrass conservation. Biol. Conserv. 100, 115–123. https://doi.org/10.1016/S0006-3207(00)00212-3.

Borfecchia, F., Micheli, C., De Cecco, L., Sannino, G., Struglia, M.V., Di Sarra, A.G., Gomez, C., Mattiazzo, G., 2021. Satellite multi/hyper spectral HR sensors for mapping the *Posidonia oceanica* in South Mediterranean islands. Sustainability 13, 13715. https://doi.org/10.3390/su132413715.

Boström, C., Baden, S., Bockelmann, A., Dromph, K., Frederiksen, S., Gustafsson, C., Krause-Jensen, D., Möller, T., Laurentis, S., Olesen, B., Olsen, J., Pihl, L., Rinde, E., 2014. Distribution, structure, and function of Nordic eelgrass (*Zostera marina*) ecosystems: implications for coastal management and conservation. Aquat. Conserv. 24 (3), 410–434. https://doi.org/10.1002/aqc.2424.

Cacabelos, E., Gestoso, I., Ramalhosa, P., Canning-Clode, J., 2022. Role of non-indigenous species in structuring benthic communities after fragmentation events: an experimental approach. Biol. Invasions 24, 2181–2199. https://doi.org/10.1007/s10530-022-02768-9.

Chatting, M., Al-Maslamani, I., Walton, M., Skov, M.W., Kennedy, H., Husrevoglu, Y.S., Le Vay, L., 2022. Future mangrove carbon storage under climate change and deforestation. Front. Mar. Sci. 9, 781876 https://doi.org/10.3389/fmars.2022.781876.

Chen, Z., Jiang, C., Nepf, H., 2013. Flow adjustment at the leading edge of a submerged aquatic canopy. Water Resour. Res. 49, 5537–5551. https://doi.org/10.1002/wrcr.20403.

Colomer, J., Ross, J.A., Casamitjana, X., 1998. Sediment entrainment in karst basins. Aquat. Sci. 60, 338–358. https://doi.org/10.1007/s000270050045.

Colomer, J., Soler, M., Serra, T., Casamitjana, X., Oldham, C., 2017. Impact of anthropogenically created canopy gaps on wave attenuation in a Posidonia oceanica seagrass meadow. Mar. Ecol. Prog. Ser. 569, 103–116. https://doi.org/10.3354/meps12090.

Colomer, J., Serra, T., 2021. The world of edges in submerged vegetated marine canopies: from patch to canopy scale. Water 13, 2430. https://doi.org/10.3390/w13172430.

Cornacchia, L., Licci, S., Nepf, H., Folkard, A., van der Wal, D., van de Koppel, J., Puijalon, S., Bouma, T.J., 2019. Turbulence-mediated facilitation of resource uptake in patchy stream macrophytes. Limnol. Oceanogr. 2, 714–727. https://doi.org/10.1002/lno.11070.

Cox, J.R., Paauw, M., Nienhuis, J.H., Dunn, F.E., van der Deijl, E., Espositio, C., Goichot, M., Leuven, J.R.F.W., van Maren, D.S., Middelkoop, H., Naffaa, S., Rahman, M., Schwarz, C., Sieben, E., Triyanti, A., Yuill, B., 2022. A global syntesis of the effectiveness of sedimentation-enchancing strategies for river deltas and estuaries. Global. Planet. Change. 214, 103796. https://doi.org/10.1016/j.gloplacha.2022.103796.

Dunn, F.E., Darby, S.E., Nicholls, R.J., Cohen, S., Zarfi, C., Fekete, B.M., 2019. Projections of declining fluvial sediment delivery to major deltas worldwide in respone to climate change and anthropogenic stress. Environ. Res. Lett. 14 (084034) https://doi.org/10.1088/1748-9326/ab304e.

Ettinger, C.L., Voerman, S.E., Lang, J.M., Stachowicz, J.J., Eisen, J.A., 2017. Microbial communities in sediment from *Zostera marina* patches, but not the Z. marina leaf or root microbiomes, vary in relation to distance from patch edge. PeerJ 5, e3246. https://doi.org/10.7717/peerj.3246.

Francalaci, S., Paris, E., Solari, L., 2021. On the prediction of settling velocity for plastic particles of different shapes. Environ. Pollut. 290, 118068 https://doi.org/10.1016/j.envpol.2021.118068.

Gacia, E., Duarte, C.M., 2001. Sediment retention by a mediterranean *Posidonia oceanica* meadow: the balance between deposition and resuspension. Estuar. Coast Shelf Sci. 52, 505–514. https://doi.org/10.1006/ecss.2000.0753.

Ganthy, F., Soissons, L., Sauriau, P.-G., Verney, R., Sottolichio, A., 2015. Effects of short flexible seagrass *Zostera noltei* on flow, erosion and deposition processes determined using flume experiments. Sedimentology 62, 997–1023. https://doi.org/10.1111/sed.12170.

García-Redondo, V., Bárbara, I., Díaz-Tapia, P., 2019. *Zostera marina* meadows in the northwestern Spain: distribution, characteristics, and anthropogenic pressures. Biodivers. Conserv. 28, 1743–1757. https://doi.org/10.1007/s10531-019-01753-4.

Gera, A., Pagès, J., Romero, J., Alcoverro, T., 2013. Combined effects of fragmentation and herbivory on *Posidonia oceanica* seagrass ecosystems. J. Ecol. 101, 1053–1061. https://doi.org/10.1111/1365-2745.12109.

Ghisalberti, M., Nepf, H., 2002. Mixing layers and coherent structures in vegetated aquatic flows. J. Geophys. Res. 107, C23011 https://doi.org/10.1029/2001JC000871.

Goring, D.G., Nikora, V.I., 2002. Despiking acoustic Doppler velocimeter data. J. Hydraul. Eng. 128 (1), 117–126.

Granata, T.C., Serra, T., Colomer, J., Casamitjana, X., Duarte, C.M., Gacia, E., 2001. Flow and particle distributions in a nearshore seagrass meadow before and after a storm. Mar. Ecol. Prog. Ser. 218, 95–106. https://doi.org/10.3354/meps218095.

Hovel, K.A., Duffy, J.E., Stachowicz, J.J., Reynolds, P., Boström, C., Boyer, K.E., Cimon, S., Cusson, M., Fodrie, F.J., Gagnon, K., Hereu, C.M., Hori, M., Jorgensen, P., Kruschel, C., Lee, K.-S., Nakaoka, M., O'Connor, N.E., Rossi, F., Ruesink, J., Tomas, F., Ziegler, S., 2021. Joint effects of patch edges and habitat degradation on faunal predation risk in a widespread marine foundation species. Ecology 102, e03316. https://doi.org/10.1002/ecy.3316, 2021.

Lera, S., Nardin, W., Sanford, L., Palinkas, C., Guercio, R., 2019. The impact of submersed aquatic vegetation on the development of river mouth bars. Earth Surf. Process. Landforms 44, 1494–1506. https://doi.org/10.1002/esp.4585.

Leriche, A., Pasqualini, V., Boudouresque, C.F., Bernard, G., Bonhomme, P., Clabaut, P., Denis, J., 2006. Spatial, temporal, and structural variations of a *Posidonia oceanica* seagrass meadow facing human activities. Aquat. Bot. 84, 287–293. https://doi.org/10.1016/j.aquabot.2005.10.001.

Liu, W.C., Liu, H.M., Young, C.C., 2022. Effects of environmental factors on suspended sediment plumes in the continental shelf out of Danshuei River Estuary. Water 14, 2755. https://doi.org/10.3390/w14172755.

López-y-Royo, C., Pergent, G., Alcoverro, T., Buia, M.C., Casazza, G., Martínez-Crego, B., Pérez, M., Silvestres, F., Romero, J., 2011. The seagrass *Posidonia oceanica* as an indicator of coastal water quality: experimental intercalibration of classification systems. Ecol. Indicat. 11, 557–563. https://doi.org/10.1016/j.ecolind.2010.07.012.

Lowe, R.J., Koseff, J.R., Monismith, S.G., 2005. Oscillatory flow through submerged canopies: 1. Velocity structure. J. Geophys. Res. 110, C10016 https://doi.org/10.1029/2004JC002788.

Luhar, M., Coutu, S., Infantes, E., Fox, S., Nepf, H., 2010. Wave-induced velocity inside a model seagrass bed. J. Geophys. Res. 115, C12005 https://doi.org/10.1029/2010JC006345.

Madsen, J.D., Chambers, P.A., James, W.F., Koch, E.W., Westlake, D.F., 2001. The interaction between water movement, sediment dynamics and submersed macrophytes. Hydrobiologia 444, 71–84. https://doi.org/10.1023/A:1017520800568.

Marin-Diaz, B., Bouma, T.J., Infantes, E., 2020. Role of eelgrass on bed-load transport and sediment resuspension under oscillatory flow. Limnol. Oceanogr. 65, 426–436. https://doi.org/10.1002/lno.11312.

Mazarrasa, I., Samper-Villareal, J., Serrano, O., Lavery, P.S., Lovelock, C.E., Marbà, N., Duarte, C.M., Cortés, J., 2018. Habitat characteristics provide insights of carbon storage in seagrass meadows. Mar. Pollut. Bull. 134, 106–117. https://doi.org/10.1016/j.marpolbul.2018.01.059.

Montefalcone, M., Bianchi, C.N., Morri, C., Peirano, A., Albertelli, G., 2006. Lower limit typology and functioning of six *Posidonia oceanica* meadows in the Ligurian Sea (NW Mediterranean). Biol. Mar. Mediterr. 13, 262–266.

Montefalcone, M., Parravicini, V., Vacchi, M., Albertelli, G., Ferrari, M., Morri, C., Bianchi, C.N., 2010. Human influence on seagrass habitat fragmentation in NW Mediterranean Sea. Estuar. Coast Shelf Sci. 86, 292–298. https://doi.org/10.1016/j.ecss.2009.11.018.

Montefalcone, M., Vacchi, M., Archetti, R., Ardizzone, G., Astruch, P., Bianchi, C.N., Calvo, S., Criscoli, A., Fernández-Torquemada, Y., Luzzu, F., Misson, G., Morri, C., Pergent, G., Tomasello, A., Ferrari, M., 2019. Geospatial modelling and map analysis allowed measuring regression of the upper limit of *Posidonia oceanica* seagrass meadows under human pressure. Estuar. Coast Shelf Sci. 217, 148–157. https://doi.org/10.1016/j.ecss.2018.11.006.

Moore, E.C., Hovel, K.A., 2010. Relative influence of habitat complexity and proximity to patch edges on seagrass epifaunal communities. Oikos 119, 1299–1311. https://doi.org/10.1111/j.1600-0706.2009.17909.x.

Navarrete-Fernández, T., Bermejo, R., Hernández, I., Deidun, A., Andreu-Cazenave, M., Cózar, A., 2022. The role of seagrass meadows in the coastal trapping of litter. Mar. Pollut. Bull. 174, 113299 https://doi.org/10.1016/j.marpolbul.2021.113299.

Olesen, B., Sand-Jensen, K., 1994. Patch dynamics of eelgrass *Zostera marina*. Mar. Ecol. Prog. Ser. 106, 147–156. https://doi.org/10.3354/meps106147.

Oreska, M.P.J., McGlathery, K.J., Porter, J.H., 2017. Seagrass blue carbon spatial patterns at the meadow-scale. PLoS One 12, e0176630. https://doi.org/10.1371/joucnal.pone.0176630.

Pastor, A., Ospina-Alvarez, A., Larsen, J., Hansen, F.T., Krause-Jensen, D., Maar, M., 2022. A network analysis of connected biophysical pathways to advice eelgrass (*Zostera marina*) restoration. Mar. Environ. Res. 179, 105690 https://doi.org/10.1010/j.marenvres.2022.105690.

Paladini de Mendoza, F., Fontolan, G., Mancini, E., Scanu, E., Scanu, S., Bonamano, S., Marcelli, M., 2018. Sediment dynamics and resuspension processes in a shallow-water *Posidonia oceanica* meadow. Mar. Geol. 404, 174–186. https://doi.org/10.1016/j.margeo.2018.07.006.

Pinheiro, L.M., Britz, L.M.K., Agostini, V.O., Pérez-Parada, A., García-Rodríguez, F., Galloway, T.S., Pinho, G.L.L., 2002. Salt marshes as the final watershed fate for meso- and microplastic contamination: a case study from Southern Brazil. Sci. Total Environ. 838, 156077 https://doi.org/10.1016/j.scitotenv.2022.156077.

Pitarch, J., Falcini, F., Nardin, W., Brando, V.E., Di Cicco, A., Marullo, S., 2019. Linking flow-stream variability to grain size distribution of suspended sediment from a satellite-based analysis of the Tiber River plume (Tyrrhenian Sea). Sci. Rep. 9, 19729 https://doi.org/10.1038/s41598-019-56409-8.

Pujol, D., Casamitjana, X., Serra, T., Colomer, J., 2013. Canopy-scale turbulence under oscillatory flow. Continent. Shelf Res. 66, 9–18. https://doi.org/10.1016/j.jhydrol.2013.01.024.

Ros, A., Colomer, J., Serra, T., Pujol, D., Soler, M., Casamitjana, X., 2014. Experimental observations on sediment resuspension within submerged model canopies under oscillatory flow. Continent. Shelf Res. 91, 220–231. https://doi.org/10.1016/j.csr.2014.10.004.

Sand-Jensen, K., Mebus, J.R., 1996. Fine-scale patterns of water velocity within macrophyte patches in streams. Oikos 76, 169–180. https://doi.org/10.2307/3545759.

Sand-Jensen, K., Pedersen, M.L., 2008. Streamlining of plant patches in streams. Freshw. Biol. 53, 714–726. https://doi.org/10.1111/j.1365-2427.2007.01928.x.

Serra, T., Colomer, J., Gacia, E., Soler, M., Casamitjana, X., 2002. Effects of a turbid hydrothermal plume on the sedimentation rates in a karstic lake. Geophys. Res. Lett. 29 (21), 1–4. https://doi.org/10.1029/2002GL015368.

Serra, T., Oldham, C., Colomer, J., 2018. Local hydrodynamics at edges of marine canopies under oscillatory flow. PLoS One 13 (8), e0201737. https://doi.org/10.1371/journal.pone.0201737.

Serra, T., Gracias, N., Hendriks, I.E., 2020. Fragmentation in seagrass canopies can alter hydrodynamics and sediment deposition rates. Water 12 (12), 3473. https://doi.org/10.3090/w12123473.

Serra, T., Colomer, J., Cristina, X., Vila, X., Arellano, J.B., Casamitjana, X., 2001. Evaluation of a laser in situ scattering instrument for measuring concentration of phytoplankton, purple sulfur bacteria, and suspended inorganic sediments in lakes. J. Environ. Eng. 127, 1023–1030. https://doi.org/10.1061/(ASCE)0733-9372(2001)127:11(1023).

Soler, M., Serra, T., Folkard, A., Colomer, J., 2021. Hydrodynamics and sediment deposition in turbidity currents: comparing continuous and patchy vegetation canopies, and the effects of water depth. J. Hydrol. 594, 125750 https://doi.org/10.1016/j.jhydrol.2020.125750.

Sweatman, J.L., Layman, C.A., Fourqurean, J.W., 2017. Habitat fragmentation has some impacts on aspects of ecosystem functioning in a sub-tropical seagrass bed. Mar. Environ. Res. 126, 95–108. https://doi.org/10.1016/j.marenvres.2017.02.003.

Tassan, S., 1997. A numerical model for the detection of sediment concentration in stratified river plumes using Thematic Mapper data. Int. J. Rem. Sens. 18 (12), 2699–2705. https://doi.org/10.1080/014311697217567.

Tuck, M.E., Ford, M.R., Kench, P.S., Masselink, G.M., 2021. Sediment supply dampens the erosive effects of sea-level rise on reef islands. Sci. Rep. 11, 5523. https://doi.org/10.1038/s41598-021-85076-x.

Valero, M., Tena, J., Torres, J., Royo, M., 2009. Estudio de la Pradera de *Posidonia oceanica (L.) Delile* del Área Litoral del Municipio de Teulada (Alicante). Nereis 2, 29–39.

van Katwijk, M.M., Bos, A.R., Hermus, D.C.R., Suykerbuyk, W., 2010. Sediment modification by seagrass beds: muddification and sandification induced by plant cover and environmental conditions. Estuar. Coast Shelf Sci. 89, 175–181. https://doi.org/10.1016/j.ecss.2010.06.008.

Van De Koppel, J., Bouma, T.J., Herman, P.M.J., 2015. The influence of local-and landscape-scale processes on spatial self-organization in estuarine ecosystems. J. Exp. Biol. 215, 962–967. https://doi.org/10.1242/jeb.060467, 2015.

Verdura, J., Santamarís, J., Ballesteros, E., Smale, D.A., Cefalì, M.E., Golo, R., de Caralt, S., Vergés, A., Cebrian, E., 2021. Local-scale climatic refugia offer sanctuary for a habitat-forming species during a marine heatwave. J. Ecol. 109, 1758–1773. https://doi.org/10.1111/1365-2745.13599.

Warrick, J.A., Mertes, L.A.K., Siegel, D.A., MacKenzie, C., 2004. Estimating suspended sediment concentrations in turbid coastal waters of the Santa Barbara Channel with SeaWiFS. J. Remote Sens. 25, 1995–2002. https://doi.org/10.1080/01431160310001619535.

Zhang, Y., Tang, C., Nepf, H., 2018. Turbulent kinetic energy in submerged model canopies under oscillatory flow. Water Resour. Res. 54, 1734–1750. https://doi.org/10.1002/2017WR021732.

Zhu, Q., Wiberg, Q., Reidenback, M.A., 2021. Quantifying seasonal seagrass effects on flow and sediment dynamics in a back-barrier bay. J. Geophys. Res.-Oceans 1, 126. https://doi.org/10.1029/2020JC016547 e2020JC016547.

Zong, L., Nepf, H., 2011. Spatial distribution of deposition within a patch of vegetation. Wat. Resour. Res 2011 47, W03516. https://doi.org/10.1029/2010WR009516.